

State of Charge Estimation of Li-ion Batteries Based on Adaptive Extended Kalman Filter

Monowar Hossain, *Student Member, IEEE*, M. E. Haque, *Senior Member, IEEE*, S. Saha, *Member, IEEE*, M.T Arif, *Member, IEEE*, AMT. Oo, *Senior Member, IEEE*
Renewable Energy and Energy Storage (REES) Research Group
School of Engineering, Deakin University, VIC 3220, Australia.
hossainm@deakin.edu.au

Abstract— The extended Kalman filter (EKF) is widely adopted for the state-of-charge (SOC) estimation of batteries. The trial and error selection of noise covariance and variation of operating temperatures lead to convergence uncertainty and poor robustness of the EKF. This paper presents an adaptive EKF (AEKF) for online SOC estimation of lithium-ion batteries based on the Thevenin equivalent circuit model (ECM) that can mitigate the problems with EKF. The parameters of the first-order Thevenin ECM are estimated using the recursive least square (RLS) method at different operating temperatures. A pulse discharge test with lithium-iron-phosphate cell has been carried out in the LabVIEW platform, where SOC of the cell is determined by the coulomb counting method (CCM). Then the SOC is estimated using the EKF and AEKF methods and compared with the CCM method. The simulation and experimental results confirm that the AEKF shows better performance compared to the conventional EKF method.

Index Terms— Li-ion battery; recursive least-square; state of charge; temperature effect; adaptive extended Kalman filter.

I. INTRODUCTION

The state-of-charge (SOC) is considered as one of the most important battery performance indicators as it ensures optimal charging/discharging, safe operation, and extends the life cycles of batteries [1]. However, an accurate SOC estimation is a very challenging task due to complex electrochemical properties of the battery cell with nonlinear and distinct electrical characteristics such as charge/discharge rate, operating temperature, voltage cut-off limit, and aging [2]. The major issues associated with an accurate SOC estimation include poor accuracy, convergence uncertainty, poor robustness and complexity in online implementation [2], [3]. Thus, an accurate SOC estimation method is mandatory for the safe and efficient operation of the battery-based energy storage systems. In the existing literature, different approaches are established for SOC estimation/prediction of Li-ion batteries, for instance, simple and enhanced coulomb counting method [4], [5], open-circuit voltage (OCV) and internal resistance methods [6], [7], learning algorithms based methods [8], [9] and model-based methods (MBMs) [10]–[13].

Among them, the model-based SOC estimation methods are gaining popularity due to their better accuracy and suitability for online applications [3]. Usually, these techniques use a battery model together with the advanced nonlinear state estimation filters/observers to estimate the real-time SOC of batteries. Different battery models such as the electrochemical model (EM) [14], [15], equivalent circuit models (ECMs) [2], [10] are used for model-based approaches.

Among different ECMs, the Thevenin-based ECM is very popular because of fast execution time, suitability for online implementation, better accuracy, and ability to estimate OCV under varying current and operating conditions [16]. Moreover, this model is capable of capturing the required battery dynamics without knowing the detail electrochemical behavior of the battery [4]. In this paper, the Thevenin equivalent circuit model (ECM) is adopted as a battery model and the parameters of ECM of battery are estimated using the recursive least square (RLS) method to make it suitable for the online model parameter estimation.

Different non-linear filters such as extended Kalman filters (EKFs) [2], [17], unscented Kalman filters (UKFs) [11], particle filters (PFs) [18], and H- ∞ filters (HFs) [19], are adopted in the existing literature for the accurate SOC estimation/prediction of Li-ion batteries. A simple EKF method is used for the SOC prediction of a commercial Li-ion battery for EV applications in the literature [2], where the authors have used EKF to improve the SOC estimated by the coulomb counting method. The result presented shows that the EKF method is capable to estimate the SOC within 4% error bound. An EKF method with the internal resistance method is established for the SOC estimation in [20], where the result analysis illustrates that this hybrid method helps to improve the SOC estimation [20]. In [17], the authors have proposed an improved EKF by introducing a gain factor to estimate SOC of the vanadium redox (VR) battery. It is mentioned in this article that the standard EKF method is unable to consider the SOC boundary constraints, and its convergence is largely affected by the uncertainty of the initial value of SOC. As a result, the EKF may result in a false alarm and poor robustness. The gain factor automatically adjusts the error in output and boundary of SOC.

Recently, the adaptive EKF method is gaining popularity in model-based approaches for practical and online SOC estimation of batteries because of its superior performance [10], [12], [21]. An adaptive EKF is presented in [10], where the authors used an improved annealing method and the adaptive switch mechanism (ASM) to improve the performance of EKF. The improved annealing method is used to get the uncertain states in the model, whereas ASM is used to tune the estimation algorithm. In [22], an AEKF is adopted for the SOC prediction/estimation of Li-ion batteries. The authors reported that the traditional EKF suffers from divergence due to the selection of inaccurate predetermined noise data. To solve this problem, the authors used particle swarm optimization (PSO), recursive least square algorithm together with standard EKF. However, the online implantation

of this proposed method may be difficult due to the higher computation requirement. An AEKF and wavelet transform matrix based SOC prediction method is adopted in [12] for EV applications. The results show better performance than the traditional AEKF method. In [21], an AEKF has been established to estimate SOC of the Li-ion batteries. The authors used AEKF to estimate online OCV of the battery, and then the OCV-SOC curve is used to estimate SOC as close as possible. Although this method shows less than 2% estimation error, it is almost impossible to obtain accurate OCV of the Li-ion cells, immediately after a charge and discharge due to high hysteresis characteristics.

In summary, traditional EKF suffers from convergence uncertainty due to the selection of inaccurate predetermined noise data. In this case, noise data is chosen by the user in a trial and error process, which leads to poor robustness of the model if an appropriate value is not found. Again, the variation of operating temperature results in changes in the impedance/model parameters of the ECM that further impact negatively on the accuracy (higher error) of the SOC estimation method. As a result, the online estimation of impedance/model parameters is one of the most important tasks to get an accurate SOC at different temperatures. In this paper, an adaptive EKF (AEKF) method is developed for online SOC estimation of lithium-ion batteries based on the first-order Thevenin equivalent circuit model (ECM). Further, this paper adopts a recursive least square (RLS) method for the online estimation of model parameters of the Li-ion batteries at different operating temperatures. The impedance parameters obtained from the RLS method is used in the SOC estimation by AEKF. The main contribution of this paper includes; (i) Development of an AEKF method for online SOC estimation of Li-ion batteries, which will select appropriate noise covariance adaptively without trial and error process, (ii) Online estimation of Li-ion battery model parameters based on recursive least square (RLS) method at different operating temperatures, which are used for SOC estimation by AEKF.

II. SOC ESTIMATION APPROACH

A. Battery Modeling and Impedance Parameter Estimation

An auto-regressive model with exogenous input (ARX) needs to be established to estimate the impedance parameters of the battery using the RLS method. Fig.1 presents a Thevenin-based ECM of a battery with n^{th} RC branches.

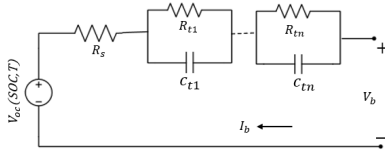


Figure 1: A Thevenin-based ECM of a Li-ion battery consisting of n^{th} RC branches.

For simplicity, consider there is a single first-order LTI system in the ECM presented in Fig.1 and its frequency-domain output voltage equation can be presented as follows [23]:

$$V_b(s) = V_{oc}(s) - V_{rs}(s) - V_{RC,1}(s) \quad (1)$$

In (1), $V_{RC,1}$ is the cell hysteresis, which is caused by the RC circuit, V_{oc} referred to as open-circuit voltage (OCV) at no-load conditions, and V_{rs} is the ohmic loss due to the instantaneous voltage drop when the battery is connected to the load. Equation (1) can be rewritten:

$$\begin{aligned} V_{oc}(s) - V_b(s) &= I_b(s) \left(R_s + \frac{1/C_1}{s + 1/R_1 C_1} \right) \\ \frac{V_{oc}(s) - V_b(s)}{I_b(s)} &= G(s) = \frac{R_s + R_1 + s R_s R_1 C_1}{1 + s R_1 C_1} \end{aligned} \quad (2)$$

In (2) $G(s)$ is the transfer function of the system. Now, the first order bilinear transformation of (2) results in:

$$G(z^{-1}) = \frac{p_2 + p_3 * z^{-1}}{1 + p_1 * z^{-1}} \Bigg|_{s \rightarrow \frac{2(1-z^{-1})}{T(1+z^{-1})}} \quad (3)$$

where,

$$\begin{aligned} p_1 &= \frac{T - 2R_1 C_1}{T + 2R_1 C_1}, p_2 = \frac{R_s T + R_1 T + 2R_s R_1 C_1}{T + 2R_1 C_1} \\ p_3 &= \frac{R_s T + R_1 T - 2R_s R_1 C_1}{T + 2R_1 C_1} \end{aligned}$$

Discretization of (3) results in:

$$\begin{aligned} V_b(k) &= V_{oc}(k) + p_1 \{V_{oc}(k-1) - V_b(k-1)\} \\ &\quad + (-p_2) I_b(k) + (-p_3) I_b(k-1) \end{aligned} \quad (4)$$

An ARX model can be established from (4) as follows:

$$\begin{cases} Y(k) = V_b(k) = \varphi^T(k) * \theta \\ \varphi(k) = [1, V_{oc}(k-1) - V_b(k-1), I_b(k), I_b(k-1)]^T \\ \theta(k) = [V_{oc}, p_1, -p_2, -p_3]^T \end{cases} \quad (5)$$

The parameters p_1 , p_2 and p_3 in (5) are identified using the RLS method. Now, the SOC estimation method requires the impedance parameters R_s , R_1 and C_1 which can be solved as follows:

$$R_1 = \frac{2(p_3 - p_1 p_2)}{1 - p_1^2}, R_s = \frac{2p_2 - R_1(1 + p_1)}{2}, C_1 = \frac{1}{2R_1} * \frac{T(1 - p_1)}{(1 + p_1)} \quad (6)$$

B. Adaptive Extended Kalman Filter (AEKF)

In the case of SOC estimation of a battery using EKF, a linear time-varying (LTV) state-space battery model is required at each time instance around the most recent SOC estimation. Once an LTV model is obtained, standard Kalman filter equations are applied. The time-domain state equations of the ECM presented in Fig.1 consist of SOC, and cell hysteresis of a first-order LTI system can be written as follows [23]:

$$\begin{aligned} SOC &= SOC_0 - \left(\frac{\eta}{C_N} \right) I_b \\ \dot{V}_{RC,1} &= - \left(\frac{1}{R_1 C_1} \right) V_{RC,1} + \left(\frac{1}{C_1} \right) I_b \end{aligned} \quad (7)$$

In (7), SOC_0 is the initial SOC of the cell, η is the columbic efficiency and C_N is the nominal capacity of the cell. In this study, columbic efficiency is considered 1. One can write, the state-space model of (7) as follows:

$$\dot{x} = A_c x + B_c u \quad (8)$$

In (8), $x \in \mathbb{R}^n$ represents the system state matrix at time t ; $u \in \mathbb{R}^p$ represents the known system input/control matrix at time t ; $A_c \in \mathbb{R}^{n \times n}$ represents the system matrix and $B_c \in \mathbb{R}^{n \times p}$ represents the input matrix. Given that, n and p are the numbers of state equations and inputs, respectively. The matrices in (8) can be obtained as follows:

$$x = \begin{bmatrix} SOC \\ V_{RC,1} \end{bmatrix}, u = \begin{bmatrix} I_b \\ I_b \end{bmatrix}, A_c = \begin{pmatrix} SOC_0 & 0 \\ 0 & -(1/R_1 C_1) \end{pmatrix}, B_c = \begin{bmatrix} -\eta/C_N \\ 1/C_1 \end{bmatrix} \quad (9)$$

Now, equation (1) can be rewritten in the time-domain format as follows:

$$V_b(t) = V_{OC}(SOC, T) - V_{TS}(i_b) - V_{RC,1}(i_b, t) \quad (10)$$

The state-space representation of (10) can be written as follows:

$$\hat{y} = C_c x + D_c u \quad (11)$$

Here, $\hat{y} \in \mathbb{R}^m$ represents the system output matrix at time t ; $C_c \in \mathbb{R}^{m \times n}$ represents the output matrix and $D_c \in \mathbb{R}^{m \times p}$ represents the input matrix. Given that m is the number of system output. The discrete state-space model for (8-11) can be written as follows:

$$x_{k+1} = A_d x_k + B_d u_k + d_k, \hat{y}_k = C_d x_k + D_d u_k + s_k \quad (12)$$

Where $d_k \in \mathbb{R}^{n \times n}$ represents system noise at time k , $s_k \in \mathbb{R}^{m \times p}$ represents the measurement noise at time k . The discretization of matrices in (12) results in:

$$A_d = \begin{pmatrix} SOC_0 & 0 \\ 0 & -\exp(T/R_1 C_1) \end{pmatrix}, B_d = \begin{bmatrix} -\eta^* T/C_N \\ R_1^* 1 - \exp(T/R_1 C_1) \end{bmatrix} \quad (13)$$

Since the Li-ion battery possesses highly nonlinear characteristics, the nonlinear form of (13) can be written as follows:

$$x_{k+1} = F(x_k, u_k) + d_k, \hat{y}_k = G(x_k, u_k) + s_k \quad (14)$$

Here, $F(x_k, u_k)$ and $G(x_k, u_k)$ are nonlinear state transition and measurement functions, respectively. In (14), the functions $F(x_k, u_k)$ and $G(x_k, u_k)$ are linearized at every time step by using Taylor first-order series expansion theorem [24] which can be written as (15-16):

$$\begin{cases} F(x_k, u_k) = F(\hat{x}_k, u_k) + \partial F(\hat{x}_k, u_k) / \partial \hat{x}_k^* (x_k - \hat{x}_k) \\ \quad = \hat{A}_k x_k + F(\hat{x}_k, u_k) - \hat{A}_k \hat{x}_k \end{cases} \quad (15)$$

$$\begin{cases} G(x_k, u_k) = G(\hat{x}_k, u_k) + \partial G(\hat{x}_k, u_k) / \partial \hat{x}_k^* (x_k - \hat{x}_k) \\ \quad = \hat{C}_k x_k + G(\hat{x}_k, u_k) - \hat{C}_k \hat{x}_k \end{cases} \quad (16)$$

Considering process and measurement noise, (15-16) can be rewritten as follows:

$$\begin{aligned} x_{k+1} &= \hat{A}_k x_k + F(\hat{x}_k, u_k) - \hat{A}_k \hat{x}_k + d_k \\ y_k &= \hat{C}_k x_k + G(\hat{x}_k, u_k) - \hat{C}_k \hat{x}_k + s_k \end{aligned} \quad (17)$$

Equations (7-17) describes the required LTV system and other matrices for the EKF implementation. The AEKF improves the EKF by incorporating the varying system uncertainty and the measurement noise adaptively using the adaptive law based on the covariance matching principle. The entire methodology for the RLS and AEKF presented in section II is summarized in Fig.2.

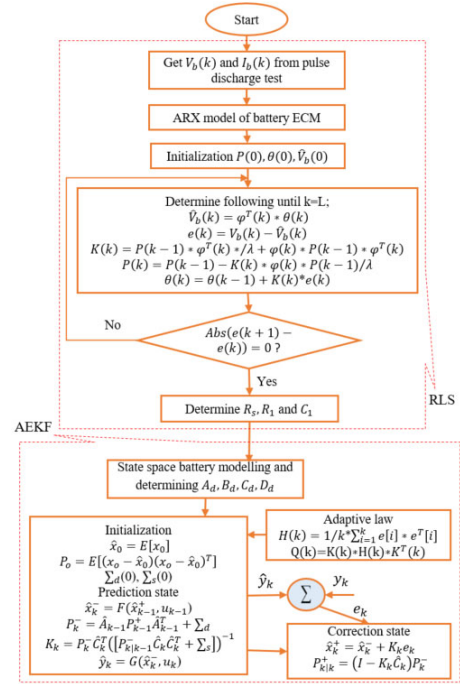


Figure 2: A combined methodology of RLS and AEKF adopted in this study.

III. RESULT AND DISCUSSION

A pulse discharge (PD) test on a new $LiFePO_4$ battery cell has been performed in the laboratory at different operating temperatures. The experimental setup for the PD test is built on the LabVIEW platform. The technical details of the cell used in the PD test are listed in Table I. A temperature-controlled incubator is used in the experiment, where PD is performed at 30 °C and 40°C. Each of the PD test periods is 360 seconds, with a 10% SOC declination step and 3600 seconds rest period. It has been programmed in LabVIEW so that the battery cell is discharged at 1C (3.34Amp) until the discharge cut-off voltage reaches (2V). The detail of the test can be found in [23].

TABLE I. TECHNICAL DETAILS OF THE CELL UNDER TEST.

Specification	Values
Cell capacity	3.34Ah@0.2C
Nominal voltage	3.2V
Charge cut-off-voltage	3.65V
Discharge cut-off-voltage	2.0V
Operating temperature	-20 °C-60 °C

The RLS method is used to predict the terminal voltage of the battery cell under test. The comparison between the voltage measured in the PD and the predicted/estimated voltage of the RLS method is presented in Fig.3. Fig.3 shows that although the RLS method has performed poorly in the first 10% SOC discharge period, the terminal voltage in the rest of the SOC discharge periods are estimated accurately. The predicted voltage with the RLS method has been used to determine the impedance parameters of the cell, such as R_s , R_l and C_l . The parameters R_s and R_l extracted from the RLS method are illustrated in Fig. 4, whereas, C_l is illustrated in Fig.5 at the operating temperature of 30 °C and 40 °C. It can be seen in Fig. 4 that as the temperature increases, the resistance decreases. It is also observed that as the SOC decrease, the resistance of the cell also decreases. As illustrated in Fig.5, the capacitance of the cell shows opposite characteristics that of resistance components of the cell. The impedance parameters obtained from the RLS method have been used in the extended Kalman filter (EKF) and adaptive EKF (AEKF) for the SOC estimation of the cell.

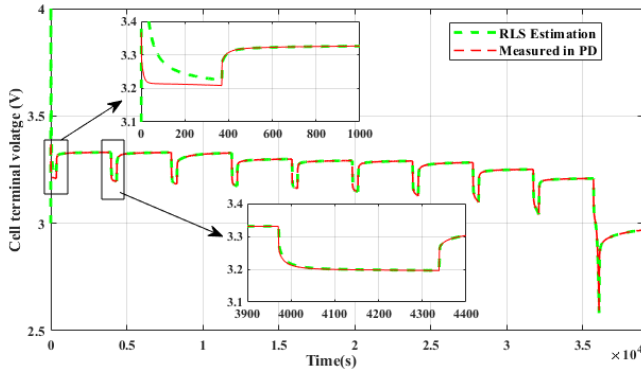


Figure 3: Comparison of measured and estimated voltage by RLS method at 30°C.

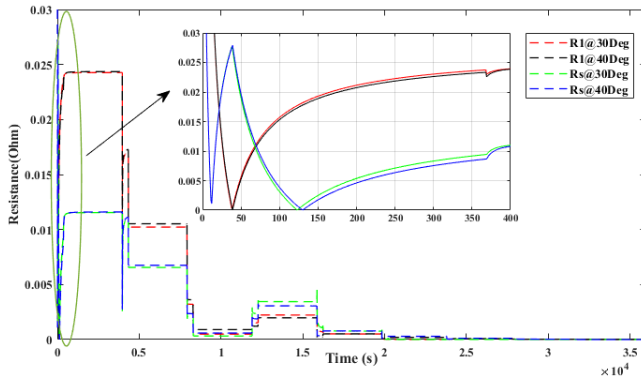


Figure 4: Resistance parameters at different operating temperatures obtained from the RLS method.

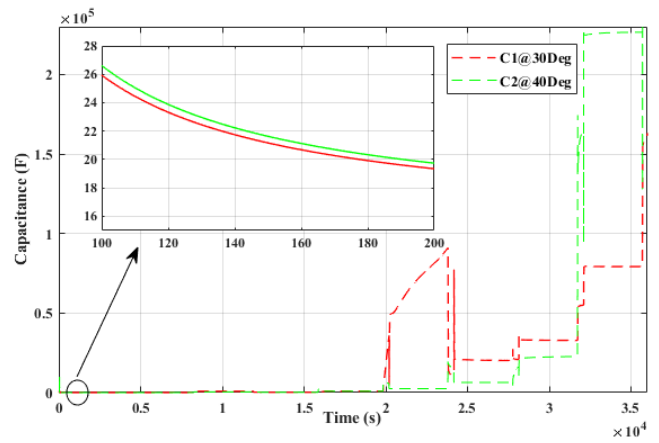


Figure 5: Capacitance parameters at different operating temperatures obtained from the RLS method.

Fig.6 shows a comparison of the SOC estimation between EKF and AEKF. The reference of the comparison is made with the SOC estimated using the Coulomb counting method in the PD test. It can be observed that as the SOC of the cell decreases (100% to 0%), the discrepancy of the SOC estimated by both EKF and AEKF increases with reference to the coulomb counting method. However, AEKF shows better agreement with the coulomb counting method than EKF. For example, in the 50% to 40% SOC discharge period, the mean absolute percentage error (MAPE) experienced by EKF and AEKF are 3.62% and 0.961%, respectively. Fig.7 shows the experimental SOC estimation by both EKF and AEKF in the custom charge and discharge test. The Coulomb counting method is used as the reference for the comparison of estimated SOC of battery. It is programmed in the LabVIEW program such that the battery cell is bound to charge and discharge between 20 to 80% of the SOC range. It can be observed that AEKF shows better agreement with the coulomb counting method than EKF. The performance analysis of both EKF and AEKF finds that the mean absolute percentage error (MAPE) experienced by EKF and AEKF is 1.214% and 0.0349%, respectively in the entire charge and discharge period. On the other hand, the percentage of root mean square error found to be 5.8% and 1.3% for EKF and AEKF respectively for the entire charge and discharge period.

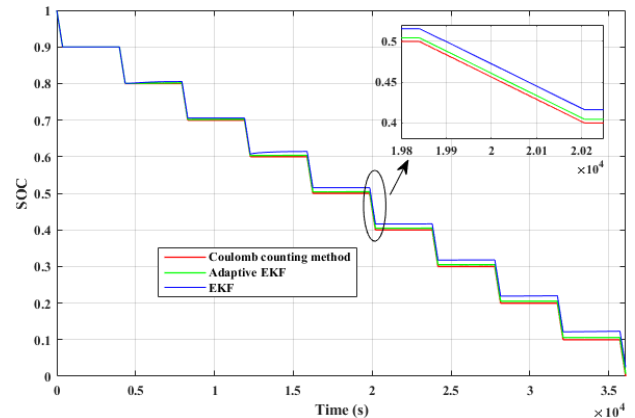


Figure 6: Experimental SOC estimation comparison at 30 °C in the pulse discharge test.

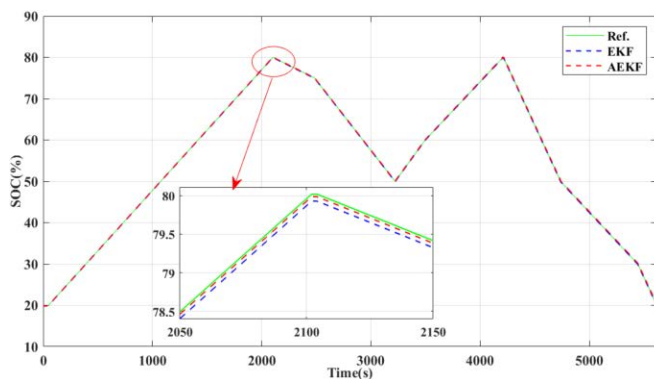


Figure 7: Experimental SOC estimation comparison at 30 °C in the custom charge and discharge test.

IV. CONCLUSIONS

This paper presents an SOC estimation approach that consists of recursive least square (RLS) and adaptive extended Kalman filter (AEKF) methods. The RLS has been adopted to identify the model parameters of the Li-ion battery at different operating temperatures, whereas the AEKF estimates the SOC of the battery using the estimated model parameters from the RLS method. The Thevenin based first-order equivalent circuit model (ECM) has been used for battery modeling in the RLS method. The analysis of the results shows that the proposed method overcomes the problems associated with traditional EKF, particularly higher convergence over time and better accuracy is achieved by the proposed method. Future works of this study will be SOC and SOH estimation of different Li-ion cells considering the effect of c-rates.

ACKNOWLEDGMENT

The authors gratefully acknowledge the contributions of Mr. James Lamont for his contribution to the experiments.

REFERENCES

- [1] K. Li, F. Wei, K. J. Tseng, and B. Soong, "A Practical Lithium-Ion Battery Model for State of Energy and Voltage Responses Prediction Incorporating Temperature and Ageing Effects," *IEEE Transactions on Industrial Electronics*, vol. 65, no. 8, pp. 6696-6708, 2018.
- [2] T. Huria, M. Ceraolo, J. Gazzarri, and R. Jackey, "Simplified extended kalman filter observer for soc estimation of commercial power-oriented lfp lithium battery cells," *SAE Technical Paper0148-7191*, 2013.
- [3] R. Xiong, J. Cao, Q. Yu, H. He, and F. Sun, "Critical Review on the Battery State of Charge Estimation Methods for Electric Vehicles," *IEEE Access*, vol. 6, pp. 1832-1843, 2018.
- [4] H. Zhang, L. Zhao, and Y. Chen, "A lossy counting-based state of charge estimation method and its application to electric vehicles," *Energies*, vol. 8, no. 12, pp. 13811-13828, 2015.
- [5] K. S. Ng, C.-S. Moo, Y.-P. Chen, and Y.-C. Hsieh, "Enhanced coulomb counting method for estimating state-of-charge and state-of-health of lithium-ion batteries," *Applied Energy*, vol. 86, no. 9, pp. 1506-1511, 2009/09/01/ 2009.
- [6] R. Xiong, Q. Yu, L. Y. Wang, and C. Lin, "A novel method to obtain the open circuit voltage for the state of charge of lithium ion batteries in electric vehicles by using H infinity filter," *Applied Energy*, vol. 207, pp. 346-353, 2017/12/01/ 2017.
- [7] Y.-H. Chiang, W.-Y. Sean, and J.-C. Ke, "Online estimation of internal resistance and open-circuit voltage of lithium-ion batteries in electric vehicles," *Journal of Power Sources*, vol. 196, no. 8, pp. 3921-3932, 2011/04/15/ 2011.
- [8] M. Luzi, M. Paschero, A. Rizzi, E. Maiorino, and F. M. F. Mascioli, "A Novel Neural Networks Ensemble Approach for Modeling Electrochemical Cells," *IEEE Transactions on Neural Networks and Learning Systems*, vol. 30, no. 2, pp. 343-354, 2019.
- [9] J. C. Á. Antón, P. J. G. Nieto, C. B. Viejo, and J. A. V. Vilán, "Support Vector Machines Used to Estimate the Battery State of Charge," *IEEE Transactions on Power Electronics*, vol. 28, no. 12, pp. 5919-5926, 2013.
- [10] Y. Shen, "Adaptive extended Kalman filter based state of charge determination for lithium-ion batteries," *Electrochimica Acta*, vol. 283, pp. 1432-1440, 2018/09/01/ 2018.
- [11] C. Huang, Z. Wang, Z. Zhao, L. Wang, C. S. Lai, and D. Wang, "Robustness Evaluation of Extended and Unscented Kalman Filter for Battery State of Charge Estimation," *IEEE Access*, vol. 6, pp. 27617-27628, 2018.
- [12] Z. Zhang, X. Cheng, Z. Lu, and D. Gu, "SOC Estimation of Lithium-Ion Batteries With AEKF and Wavelet Transform Matrix," *IEEE Transactions on Power Electronics*, vol. 32, no. 10, pp. 7626-7634, 2017.
- [13] S. Nejad, D. T. Gladwin, and D. A. Stone, "A systematic review of lumped-parameter equivalent circuit models for real-time estimation of lithium-ion battery states," *Journal of Power Sources*, vol. 316, pp. 183-196, 2016/06/01/ 2016.
- [14] A. Guha and A. Patra, "Online Estimation of the Electrochemical Impedance Spectrum and Remaining Useful Life of Lithium-Ion Batteries," *IEEE Transactions on Instrumentation and Measurement*, no. 99, pp. 1-14, 2018.
- [15] R. Gu, P. Malysz, H. Yang, and A. Emadi, "On the Suitability of Electrochemical-Based Modeling for Lithium-Ion Batteries," *IEEE Transactions on Transportation Electrification*, vol. 2, no. 4, pp. 417-431, 2016.
- [16] T. Huria, M. Ceraolo, J. Gazzarri, and R. Jackey, "High fidelity electrical model with thermal dependence for characterization and simulation of high power lithium battery cells," in *2012 IEEE International Electric Vehicle Conference*, 2012, pp. 1-8.
- [17] Y. Qiu, X. Li, W. Chen, Z.-m. Duan, and L. Yu, "State of charge estimation of vanadium redox battery based on improved extended Kalman filter," *ISA Transactions*, 2019/04/20/ 2019.
- [18] M. Ye, H. Guo, R. Xiong, and R. Yang, "Model-based State-of-charge Estimation Approach of the Lithium-ion Battery Using an Improved Adaptive Particle Filter," *Energy Procedia*, vol. 103, pp. 394-399, 2016/12/01/ 2016.
- [19] C. Lin, H. Mu, R. Xiong, and W. Shen, "A novel multi-model probability battery state of charge estimation approach for electric vehicles using H-infinity algorithm," *Applied Energy*, vol. 166, pp. 76-83, 2016/03/15/ 2016.
- [20] D. Wang, Y. Bao, and J. Shi, "Online Lithium-Ion Battery Internal Resistance Measurement Application in State-of-Charge Estimation Using the Extended Kalman Filter," *Energies*, vol. 10, no. 9, p. 1284, 2017.
- [21] R. Xiong, H. He, F. Sun, and K. Zhao, "Evaluation on State of Charge Estimation of Batteries With Adaptive Extended Kalman Filter by Experiment Approach," *IEEE Transactions on Vehicular Technology*, vol. 62, no. 1, pp. 108-117, 2013.
- [22] X. Yu, J. Wei, G. Dong, Z. Chen, and C. Zhang, "State-of-charge estimation approach of lithium-ion batteries using an improved extended Kalman filter," *Energy Procedia*, vol. 158, pp. 5097-5102, 2019/02/01/ 2019.
- [23] M. Hossain, S. Saha, M. Haque, M. Arif, and A. Oo, "A Parameter Extraction Method for the Thevenin Equivalent Circuit Model of Li-ion Batteries," in *2019 IEEE Industry Applications Society Annual Meeting*, pp. 1-7: IEEE.
- [24] J. E. Marsden and A. Tromba, *Vector calculus*. Macmillan, 2003.